Available online at www.sciencedirect.com
ScienceDirect
Developmental Biology 313 (2008) 648–658
DEVELOPMENTAL BIOLOGY
www.elsevier.com/developmentalbiology

The role of Slit-Robo signaling in the generation, migration and morphological differentiation of cortical interneurons

William Andrews [a,*,1], Melissa Barber [a,1], Luis R. Hernadez-Miranda [a], Jian Xian [b], Sonja Rakic [a], Vasi Sundaresan [c], Terence H. Rabbitts [d,e], Richard Pannell [d], Pamela Rabbitts [e], Hannah Thompson [f], Lynda Erskine [f], Fujio Murakami [g], John G. Parnavelas [a]

[a] *Department of Anatomy and Developmental Biology, University College London, Gower Street, London WC1E 6BT, UK*
[b] *Department of Oncology, Hutchinson-MRC Research Centre, Cambridge, UK*
[c] *Princess Alexandra NHS Trust, Harlow, UK*
[d] *Laboratory of Molecular Biology, MRC Centre Hills Road, Cambridge, UK*
[e] *Leeds Institute of Molecular Medicine, St. James's University Hospital, Leeds, UK*
[f] *Division of Visual Science and Molecular Genetics, Institute of Ophthalmology, University College London, UK*
[g] *Osaka University, Osaka, Japan*

Received for publication 3 July 2007; revised 12 October 2007; accepted 31 October 2007
Available online 13 November 2007

Abstract

Cortical interneurons in rodents are generated in the ventral telencephalon and migrate tangentially into the cortex. This process requires the coordinated action of many intrinsic and extrinsic factors. Here we show that Robo1 and Robo2 receptor proteins are dynamically expressed throughout the period of corticogenesis and colocalize with interneuronal markers, suggesting that they play a role in the migration of these cells. Analysis of Robo mutants showed a marked increase in the number of interneurons in the cortices of Robo1$^{-/-}$, but not Robo2$^{-/-}$, animals throughout the period of corticogenesis and in adulthood; this excess number of interneurons was observed in all layers of the developing cortex. Using BrdU incorporation in dissociated cell cultures and phosphohistone-3 labeling *in vivo*, we demonstrated that the increased number of interneurons in Robo1$^{-/-}$ mice is, at least in part, due to increased proliferation. Interestingly, a similar increase in proliferation was observed in Slit1$^{-/-}$/Slit2$^{-/-}$ mutant mice, suggesting that cell division is influenced by Slit-Robo signaling mechanisms. Morphometric analysis of migrating interneurons in Robo1$^{-/-}$, Robo2$^{-/-}$ and Slit1$^{-/-}$/Slit2$^{-/-}$, but not in Slit1$^{-/-}$ mice, showed a differential increase in neuronal process length and branching suggesting that Slit-Robo signaling also plays an important role in the morphological differentiation of these neurons.

Keywords: Robo; Slit; Interneuron; Morphology

Introduction

The origins and migratory routes of cortical interneurons in rodents are now well documented. Tracing studies have confirmed that these cells arise in different parts of the ganglionic eminence (GE) in the ventral telencephalon and migrate in tangentially oriented streams to enter the cortex (Corbin et al., 2001; Marín and Rubenstein, 2003; Métin et al., 2006). At the early stages of corticogenesis (E12.5 in mouse), they appear almost exclusively in the preplate layer (PPL), while at later embryonic ages the streams are at the levels of the intermediate zone (IZ)/subventricular zone (SVZ), marginal zone (MZ) and subplate (SP; after the split of the PPL). Once in the cortex, they leave their migratory streams to assume positions in the cortical plate (CP) where they assemble into functional circuits with their pyramidal counterparts, contributing to a precise balance of synaptic excitation and inhibition in the cortex. It has been suggested that disruption of this balance results in neuropathological conditions such as epilepsy and Parkinson's disease (Sloviter, 1987; Cobos et al., 2005; Kumar and Buckmaster, 2006; Mallet et al., 2006).

* Corresponding author. Fax: +44 20 7679 7349.
E-mail address: w.andrews@ucl.ac.uk (W. Andrews).
[1] Both authors contributed equally to this manuscript.

0012-1606/$ - see front matter © 2007 Elsevier Inc. All rights reserved.
doi:10.1016/j.ydbio.2007.10.052

The molecular mechanisms that guide the migration of interneurons from the GE, around the corticostriatal notch and into the cortex are the subject of continuing investigations, but a number of molecules have already been demonstrated to play important roles (Nadarajah and Parnavelas, 2002; Marín and Rubenstein, 2003; Métin et al., 2006). These include the Slit proteins and their receptors of the Robo family (Andrews et al., 2006). Evidence from *in vitro* experiments indicates that the migration of interneurons is initiated by the chemorepulsive activity of Slit secreted from the ventricular zone (VZ) of the GE (Hu, 1999; Wu et al., 1999; Zhu et al., 1999). However, it has been reported that migration of cortical interneurons is normal in Slit1$^{-/-}$/ Slit2$^{-/-}$ mutants, prompting speculation that Slits do not play a major role in tangential migration (Marín et al., 2003; Marín and Rubenstein, 2003). In an attempt to investigate whether Robo receptors are involved in this process, we recently analyzed the phenotype of Robo1$^{-/-}$ mice. We noted, in addition to abnormalities in the formation of major axonal tracts, a significant increase in the number of interneurons that enter the cortex from the ventral forebrain throughout the period of corticogenesis (Andrews et al., 2006). This shows that Robo1$^{-/-}$ mice have a different phenotype from Slit mutants, suggesting that additional ligands, receptors or receptor partners are likely to be involved in these processes.

In addition to regulating axon guidance and cell migration, Slit-Robo signaling plays a role in process outgrowth and branching. Specifically, Slit has been reported to promote axonal elongation and branching in sensory neurons (Wang et al., 1999; Ozdinler and Erzurumlu, 2002; Ma and Tessier-Lavigne, 2007) and dendritic growth and branching in cortical cells (Whitford et al., 2002). Furthermore, Slit has been found to promote branching and elongation of neurites of GABA-containing interneurons in embryonic forebrain cultures (Sang et al., 2002).

In the present study, we investigated the role of Slit-Robo signaling in the generation and migration of cortical interneurons and in their morphological differentiation. We first analyzed the localization of Robo1 and Robo2 in the developing forebrain and found that these proteins show complementary and dynamic patterns of expression throughout the period of cortex formation. Further, we found that both receptors are expressed in cortical interneurons during corticogenesis, suggesting that they may play a role in their migration. Analysis of Robo1$^{-/-}$ and Robo2$^{-/-}$ animals showed no change in the positions of the streams of migrating interneurons in the cortices of both groups of mice, which is similar to that reported for Slit mutants (Marín et al., 2003). However, an increased number of cells were observed in the Robo1$^{-/-}$ mutants, and this increase persisted to adulthood. In addition, we found that removal of Robo1, Robo2 or both Slit1/Slit2 (but not Slit1 alone) differentially affected the morphology of migrating interneurons. These findings demonstrate that Slit-Robo signaling plays an important role in the development of the interneuron population of the cerebral cortex.

Materials and methods

Animals

All experimental procedures were performed in accordance with the UK Animals (Scientific Procedures) Act 1986 and institutional guidelines. Wild-type animals were C57/bl6J mice obtained from Charles River Ltd. Robo2$^{-/-}$ and Slit1$^{-/-}$/ Slit2$^{-/-}$ mice were generated as described previously (Lu et al., 2007; Plump et al., 2002, respectively). Robo1 full gene (Dulox) mutant mice were generated as outlined below and in Supplementary Fig. 1. *GAD67-GFP* (Δneo) mice (Tamamaki et al., 2003; kindly provided by Drs. Y. Yanagawa and K. Obata, Japan) used in this study were also maintained in C57/bl6J background. The day the vaginal plug was found was considered as embryonic day (E) 0.5.

Generation of Robo1 (Dulox) mutant mice

A genomic library of E14 TG2α embryonic stem (ES) cell DNA was screened with a mouse Robo1 cDNA clone corresponding to exon 1 and exon 22, and positive clones were purified and subcloned into pBlucecript. A 5.4-kb *Bam*HI fragment containing exon 1 of the mouse *Robo1* gene and a 7.0-kb *Xba*I fragment containing exon 22 of the same gene were used for construction of the targeting vectors. Each construct comprised a selection marker gene (PGK*hyg*pA or PGK*puro*pA) and a *loxP* sequence to enable Cre-mediated recombination events. The vectors were designed for positive–negative selection of targeted cells and contained a thymidine kinase gene expression cassette at the end of one of the homology arms. The final vectors were linearized with *Xho*I for electroporation. Twenty-five micrograms of exon 1 targeting vector linearized with *Xho*I was electroporated into 1×10^7 CCB ES cells, and cells were selected in hygromycin B (125 μg/ml) and ganciclovir (2.5 μM). Targeted clones were identified by Southern blotting of *Xba*I-digested DNA and hybridization with an exon 1 probe corresponding to a sequence external to the vector homology arm (probe a). Southern blotting was carried out as described previously by Xian et al. (2001).

In the second transfection, the exon 22 targeting vector linearized with *Xho*I was electroporated into 1×10^7 cells of the exon 1 targeted cell line derived from the first round of transfection, and cells were selected in puromycin (0.5 μg/ml) and ganciclovir. Targeted clones were identified by Southern blotting of *Xba*I-digested DNA and hybridization with an exon 22 probe corresponding to a sequence external to the vector homology arm (probe b). ES cells from two independent clones were used for injection into blastocysts derived from C57/bl6J mice. Blastocysts were transferred to pseudo-pregnant females, and chimeric offspring were detected by the presence of agouti colour on a non-agouti background. Chimeric males were mated to C57/bl6J females to produce ES cell-derived offspring. Their genotype was confirmed by Southern blot analysis of tail DNA. Mice heterozygous for the gene-targeting event – i.e., deletions of the whole Robo1 gene – were intercrossed to generate homozygotes.

Immunohistochemistry

Embryonic brains (E13.5–E18.5) were fixed in 4% paraformaldehyde (PFA) in phosphate-buffered saline (PBS) for 4–8 h, depending on the age of the embryos. Adult mice were perfused with 4% PFA, and their brains were removed and immersed in fixative solution overnight. Brains were subsequently cryoprotected in 30% sucrose in PBS, embedded in Tissue-Tek OCT (Sakura Finetek Europe, Zoeterwoude, The Netherlands) and sectioned in the coronal plane at 25 μm using a Cryostat (Bright Instruments, Huntingdon, UK). Sections were washed in PBS and blocked in a solution of 5% serum (v/v) and 0.3% Triton X-100 (v/v) (Sigma-Aldrich, Dorset, UK) in PBS for 2 h. Normal goat serum (Vector Laboratories, Burlingame, CA) or normal donkey serum (Jackson ImmunoResearch, Soham, UK) was used for primary antibodies made in mouse, rabbit or goat, respectively. Sections were incubated overnight in one of the following primary antibodies: rabbit anti-calbindin (1:10000; D-28K, Swant, Bellinzona, Switzerland); mouse anti-bromodeoxyuridine (BrdU; 1:100; Progen, Heidelberg, Germany); rabbit anti-phosphohistone 3 (1:1000; Abcam Ltd., UK); goat anti-Robo1 (1:100; R&D Systems); goat anti-Robo2 (1:100; R&D

Systems); rabbit anti-Robo1 and anti-Robo2 (1:2,000; antibodies prepared by Professor F. Murakami); and rabbit anti-ARX (1:1000; Poirier et al., 2004). They were then washed in PBS and incubated in biotinylated goat anti-mouse (1:200; Vector Laboratories), biotinylated goat anti-rabbit (1:200; Vector Laboratories) or biotinylated donkey anti-goat (1:200; Jackson Immuno-Research Laboratory) for 2 h and processed using a conventional immunohistochemistry protocol. Other secondary antibodies used were mouse anti-rabbit 488 and rabbit anti-mouse 488 (Alexa, Invitrogen Corp., UK). Robo staining was enhanced using a tyramide signal amplification system (TSA, Perkin Elmer, Boston, MA) according to manufacturer's instructions. Sections were washed and incubated with 4′-6-diamidino-2-phenyllindole (DAPI, 1:20,000; Sigma-Aldrich) in PBS or bisbenzimide (10 min in 2.5 μg/ml solution in PBS; Sigma-Aldrich). Images were collected using an SP2 Leica confocal microscope (Leica Microsystems, UK). Sequential images were subsequently reconstructed using Metamorph imaging software (Universal Imaging Corporation, West Chester, PA).

Quantification of interneuron distribution

Calbindin-positive cells were counted in coronal strips (400 μm wide) spanning the thickness of the middle (along the rostro-caudal axis) regions of the cortex at E15.5 (minimum of 8 sections from each of 3 animals for each condition). In all counts, the experimenter did not know the condition of the animal. Strips were divided into 5 bins arranged parallel to the pial surface that corresponded to the different layers of the developing cortex (VZ, SVZ/LIZ, IZ, SP, CP), from bin1 (VZ) to bin 5 (upper CP). The extent of the layers was determined by methyl green counterstaining (Vector Laboratories).

Morphometric analysis

Calbindin-positive neurons were drawn at a primary magnification of ×400 using a drawing apparatus attached to a Zeiss Photomicroscope. Morphometric parameters including number of primary processes, number of branch points and total process length for each cell were measured using imaging analysis software (ImageJ; NIH, version 1.34n) with custom made programming macros (see Supplementary Fig. 2 for details). Means and standard error of the mean (SEM) were calculated, and the differences were tested using an unpaired Student's *t* test. Significance was set at a P value of <0.05.

Dissociated cell cultures

Dissociated cell cultures were prepared from E12.5 mouse telencephalons according to the method of Cavanagh et al. (1997). Briefly, GEs were dissected from embryonic forebrains in Hanks' solution under a stereo microscope, and isolated tissue was dissociated enzymatically in Neurobasal media with trypsin (0.1%) and DNase I (0.001%) at 37 °C for 15 min. Trypsin was inactivated by 10% fetal calf serum (FCS) in Neurobasal media for 5 min, and cells were dissociated by delicate trituration with a sterile pipette tip. The resulting suspension was centrifuged at 1000×*g* for 3 min, the supernatant was discarded, and the cells were resuspended in neurobasal media containing B27 supplement, 100 μg/ml penicillin/streptomycin and 2 mM L-glutamine. They were then plated at a density of 2×10^5 cells on poly-L-lysine (10 μg/ml) and laminin (10 μg/ml)-coated 13-mm coverslips in 24-well plates. Cultures were kept in a humidified incubator (95% air/5% CO_2) at 37 °C, and cells were allowed to attach to the coverslips for 30 min. Fresh media were then added and again on the following morning.

Proliferation rate

The rate of proliferation, assessed in dissociated GE cultures derived from E12.5 mouse embryos, was determined as the proportion of calbindin-positive cells that incorporated BrdU. Cultures were pulsed with 10 μM of BrdU for 2 h in order to label as many cells in S-phase without allowing them to enter mitosis (for details, see Cavanagh et al., 1997). Cells were washed and fixed with 4%

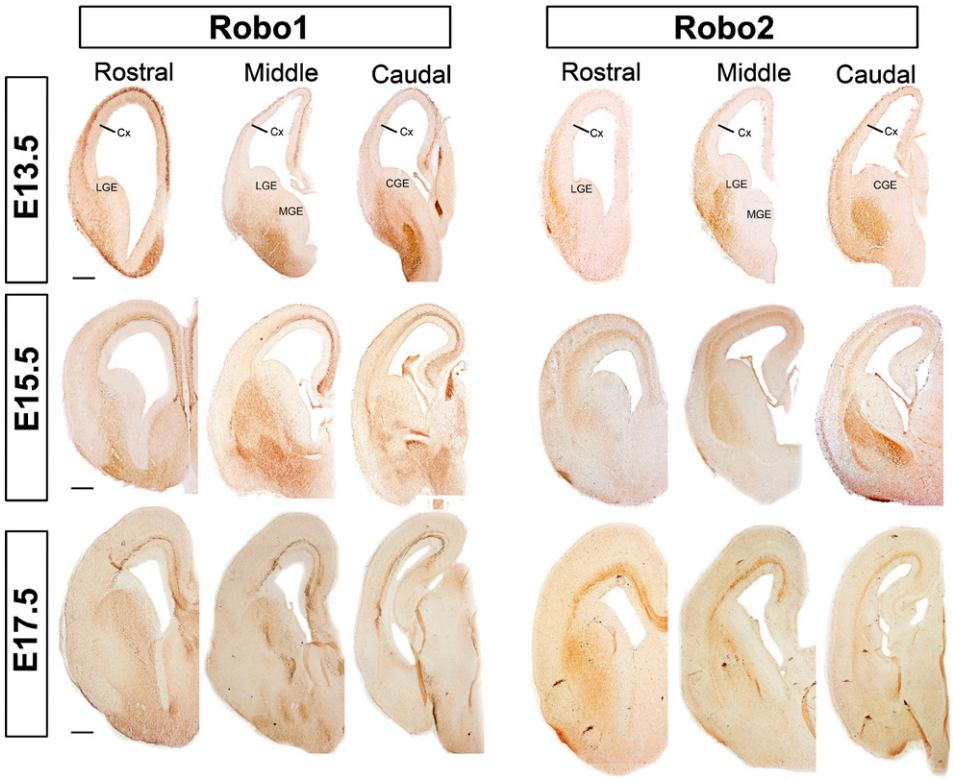

Fig. 1. Robo1 and Robo2 expression in the mouse embryonic forebrain. Immunohistochemical localization of Robo1 and Robo2 proteins in coronal sections taken at rostral, middle and caudal levels of the embryonic mouse forebrain. Robo1 and Robo2 are expressed throughout the rostro-caudal extent of the differentiating basal ganglia and cortex during early (E13.5) and later phases (E15.5, E17.5) of development. LGE, lateral ganglionic eminence; MGE, medial ganglionic eminence; CGE, caudal ganglionic eminence; Cx, Cortex. Scale bar, 300 μm.

PFA, co-immunostained for BrdU and calbindin and counterstained with DAPI. Cell counts were made with a ×40 objective in nine fields of view for each sample. Statistical significance was evaluated using Student's *t*-test.

To determine the effect of Slit on interneuron proliferation, we prepared E12.5 GE cultures from GAD67-GFP mice. These were incubated overnight in the presence or absence of 4 μg/ml recombinant mouse Slit3 (R&D Systems). Cells were washed and fixed with 4% PFA, immunostained for phosphohistone 3 and counterstained with DAPI. Cell counts were made with a ×40 objective in ten fields of view for each sample, carried out in quadruplicate.

Results

Robo protein expression during forebrain development

Robo1 and Robo2 mRNA are localized in the developing cortex and the proliferative zone of the GE (Marillat et al., 2002; Whitford et al., 2002), suggesting that these receptors may be associated with the movement of cortical interneurons away from the ventral telencephalon. Here we examined Robo1 and Robo2 protein expression patterns in coronal sections of mouse brains from early (E13.5), mid (E15.5) and late (E17.5) stages of corticogenesis. Staining for Robo1 and Robo2 was observed throughout the rostro-caudal extent of the developing forebrain at all ages examined (Fig. 1). The expression of these receptors was largely complementary within the early differentiating ventral telencephalon (E13.5; Fig. 1), with strong Robo1 staining localized throughout the mantle zone of the MGE, and Robo2 restricted more laterally to the differentiating LGE. Robo1 and Robo2 expression expanded by E15.5, overlapping to a greater degree within the differentiating basal ganglia. In the cortex, there was strong expression of both Robos throughout the PPL and in the zones that result from its splitting, the MZ and the SP, as well as in the tangential migratory routes travelled by interneurons at this developmental stage, and especially within the LIZ/SVZ. By E17.5, the expression of both Robo receptors was somewhat down regulated in the ventral telencephalon but remained strong within the SVZ of the cortex (Fig. 1).

Immunohistochemical staining of E15.5 coronal sections for Robo1 and calbindin, a marker of cortical interneurons in early development, showed that both molecules colocalize extensively in neurons throughout the cortical anlage (Fig. 2A). On closer examination, individual Robo1/calbindin double-labeled cells appeared to be leaving the SP and IZ/SVZ migratory streams and moving into the developing CP and VZ, respectively (arrows, Figs. 2B, C). Robo2 staining was confined to the upper part of the developing cortex (Fig. 2D), which was particularly strong in the SP and MZ. Similar to Robo1, individual Robo2/calbindin double-labeled interneurons were present throughout the developing cortex (Figs. 2E, F). Quantitative analysis of the proportion of calbindin-positive cells expressing either Robo protein at E15.5 revealed that more than 90% of these cells express either Robo receptor in all cortical layers, except for the VZ where 70–80% of interneurons express either receptor (Fig. 2G); similar results were obtained at E13.5 (data not shown). Thus, most interneurons appear to express both Robo receptors in all cortical layers throughout early and mid phases of corticogenesis. These observations suggest that Robo1 and Robo2 may have roles not only in the migration of interneurons from the GE, but also in their final positioning within the neocortex.

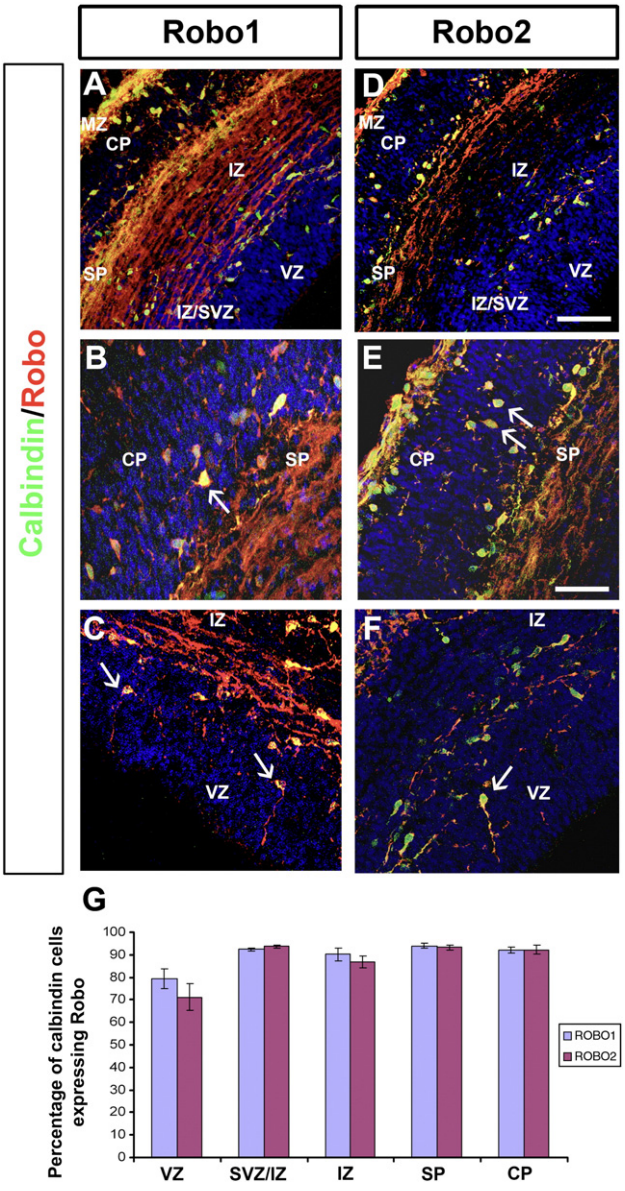

Fig. 2. Colocalization of Robo proteins with the cortical interneuron marker, calbindin. (A–F) Immunohistochemical localization of calbindin (green) and Robo1 or Robo2 (red) staining in E15.5 coronal sections through the cortex. Colocalization of calbindin and both Robo receptors (arrows) can be seen in individual cells at all levels of the developing cortex. (G) Graphic representation of the percentage of calbindin-positive cells that also express either Robo1 (blue) or Robo2 (red) in all cortical layers at E15.5. Scale bars in panel D = 100 μm in panels A, D; in panel E = 50 μm in panels B, C, E and F.

Cortical interneurons in Robo and Slit mutant mice

We have previously reported a significant increase in the number of interneurons present in the cortices of Robo1 (Exon 5 deleted) mutant (−/−) animals compared to wild-type (+/+)

littermates (Andrews et al., 2006), suggesting that Robo1 plays a role in the development of these cells. In order to further assess the roles of Slit-Robo proteins in this process, we examined the cortices of Robo1$^{-/-}$, Robo2$^{-/-}$, Slit1$^{-/-}$Slit2$^{+/+}$ and Slit1$^{-/-}$Slit2$^{-/-}$ mice. While our study was carried out on the previously described Robo2 and Slit mutant mouse strains (Lu et al., 2007; Plump et al., 2002, respectively), the Robo1 analysis was performed on the newly generated Dulox Robo1$^{-/-}$ animals, in which the whole Robo1 gene (exons 1–22 inclusive) has been fluxed and deleted (for details, see Supplementary Fig. 1). A recent study by López-Bendito et al. (2007) on the roles of Robo receptors in the guidance of the major axonal tracts in the forebrain has noted differences in the strength of cortical phenotypes between their Robo1 mutant strain and our Robo1 exon 5 deleted strain. It is possible that these differences could have arisen from

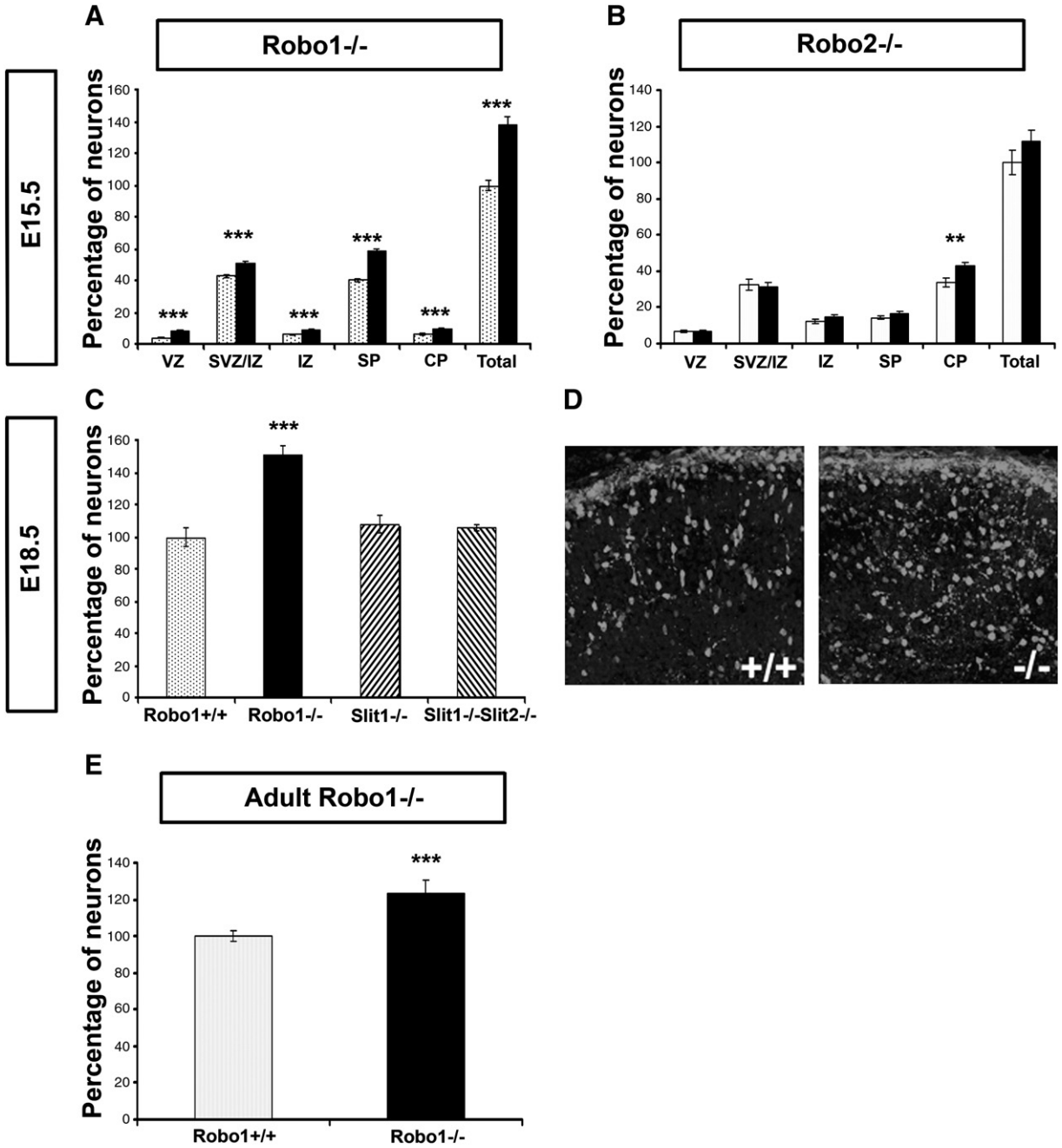

Fig. 3. Increased number of interneurons in all cortical layers in Robo1$^{-/-}$ mice. Histograms representing the total number and distribution of calbindin-positive cells in coronal sections taken through the cortices of Robo1$^{-/-}$ (A) and Robo2$^{-/-}$ (B) mice at E15.5. Values are shown as a percentage of the total number of neurons present in the cortex of control littermates in different cortical layers. An increase in the number of calbindin cells is seen in most cortical layers (VZ–CP) in both Robo mutants at E15.5, which is significant for all layers in the Robo1$^{-/-}$, and only the CP in Robo2$^{-/-}$ animals. Analysis of Robo1$^{-/-}$ and Slit mutants at E18.5 (C) showed a similarly marked increase in the number of calbindin-positive neurons in Robo1$^{-/-}$ mutants (approximately 50% increase, compared to controls), as is also apparent in the two stained sections (D); no significant differences were observed in Slit mutants (C). Cell counts in adults showed that the significantly increased number of interneurons is maintained in the cortex of Robo1$^{-/-}$ mice (E). Histograms show averages and error bars represent SEM. Student's *t*-test $^{**}p \leq 0.001$; $^{***}p \leq 0.00001$.

variations in mouse strains used or could be due to genetic alterations, resulting in their mouse line being a hypermorph rather than a true mutant. In order to avoid potentially conflicting results, we decided to produce a mouse mutant that lacks the entire Robo1 gene.

Coronal sections taken through middle (along the rostro-caudal axis) regions of the cortex at E15.5 were immunostained for calbindin, and the number and the distribution of labeled cells throughout the cortical thickness were analyzed. Our analysis showed a significant increase in the number of calbindin-positive cells in all cortical layers of Dulox Robo1$^{-/-}$ mutants, and particularly in the SP ($p \leq 8.9 \times 10^{-16}$), compared to control littermates (Fig. 3A, $n=8$ heterozygotes, Robo1$^{+/-}$, $n=7$ Robo1$^{-/-}$). This result compared favorably with our earlier findings in the Robo1 Exon 5 deletion mutant mouse (Andrews et al., 2006; $n=3$ Robo1$^{+/-}$, $n=4$ Robo1$^{-/-}$; data not shown). The significantly increased number of cortical interneurons in Dulox Robo1$^{-/-}$ mice was maintained at E18.5 (Figs. 3C, D; $n=6$, Robo1$^{+/+}$ 100±6.2%, Robo1$^{-/-}$ 151±5.7%). To assess cell numbers in adult animals, we employed ARX, another interneuron marker (Friocourt et al., 2007), as calbindin is known to label a number of cortical pyramidal cells in postnatal life. This analysis showed that the increase in interneuron numbers in the cortices of Dulox Robo1$^{-/-}$ mice does persist into adulthood (Fig. 3E; $n=3$, Robo1$^{+/+}$ 100±2.9%, Robo1$^{-/-}$ 123±6.9%).

Counts in Robo2$^{-/-}$ animals at E15.5 ($n=4$ Robo2$^{+/+}$, $n=4$ Robo2$^{-/-}$) revealed only a small increase in the number of calbindin cells restricted to the CP (Fig. 3B). However, analysis at E17.5 showed no significant changes in the number of interneurons in the cortices of Robo2$^{-/-}$ animals compared to controls ($n=4$ Robo2$^{+/+}$, $n=4$ Robo2$^{-/-}$, data not shown). Similar to Robo2$^{-/-}$ mice, analysis of Slit mutants, Slit1$^{-/-}$Slit2$^{+/+}$ or Slit1$^{-/-}$/Slit2$^{-/-}$ at E18.5 revealed no significant changes in the number of interneurons (Fig 3C; $n=2$ Slit1$^{-/-}$Slit2$^{+/+}$; $n=2$ Slit1$^{-/-}$/Slit2$^{-/-}$). Further analysis of either Robo2$^{-/-}$ or Slit double mutants at later stages was precluded as these mutants die at birth. Our results suggest that only Robo1 has a pronounced effect on the number of interneurons entering the cortex, and this increase is apparent in all layers.

Increased proliferation in Robo1$^{-/-}$ and Slit1$^{-/-}$Slit2$^{-/-}$ mutant mice

The increase in the number of calbindin-positive cells migrating into the neocortex of Robo1$^{-/-}$ mice could be due to a defect in migration and/or due to an increase in proliferation or reduction in cell death. We suggest that the latter possibility is rather unlikely in view of the fact that, overall, little apoptosis is observed in the developing and adult cortex, apart from the SVZ at birth and in the first 2 postnatal weeks (Thomaidou et al., 1997).

In order to study the potential effects on proliferation, we initially prepared dissociated cell cultures from the GEs of Robo1$^{-/-}$ mutant mice. Cultures were incubated for 18 h and then pulsed with BrdU for 2 h. These were then fixed in 4% PFA and double labeled to identify BrdU and calbindin-positive cells. Fig. 4C shows the percentage of calbindin expressing cells that are also BrdU positive in cultures prepared from mutant and control GEs. The results indicate a significant increase in the proportion of calbindin-positive cells that had incorporated BrdU in Robo1$^{-/-}$ mouse derived cultures ($n=4$; 71.2±1.4%, $p \leq 0.0017$) compared with cultures prepared from either wild-type ($n=6$; 56.5±2.4%) or heterozygote ($n=5$; 51.1±4.3%) littermates (Figs. 4A–C). Similar results were also obtained with Robo1 exon Δ5 mutants (data not shown).

In order to study this further, we assessed the proliferation rates in Robo1 and Slit mutant mice using the mitotic marker phosphohistone 3 (PH3), as changes in cell proliferation has not previously been shown for Slit mutants. Coronal sections taken through middle (along the rostro-caudal axis) regions of the cortex (E12.5–E16.5) were immunostained for PH3, and the number of labeled cells present within the ventricular zone of the GE was determined. Our analysis of Dulox Robo1 mutants at E15.5 indicated, similar to our observations *in vitro*, a marked increase in the percentage of cells that were PH3 positive ($n=3$ Robo1$^{-/-}$ 132.6±4.7%, $p \leq 0.0012$) compared to wild-type littermates ($n=3$ Robo1$^{+/+}$ 100±3.5%) (Figs. 4D–F). Similar results were obtained at E12.5 ($n=3$ Robo1$^{-/-}$; $n=3$ Robo1$^{+/+}$, data not shown). Interestingly, our analysis of Slit1$^{-/-}$Slit2$^{-/-}$ mice also revealed a significant increase in the percentage of cells that were PH3 positive ($n=3$ 138.6±4.4%, $p \leq 0.0006$) compared to Slit1$^{-/-}$Slit2$^{+/+}$ ($n=3$ 100±3.1%) littermates at E13.5 (Figs. 4G–I). Similar results were also obtained at E16.5 ($n=2$ Slit1$^{-/-}$Slit2$^{-/-}$; $n=2$ Slit1$^{-/-}$Slit2$^{+/+}$, data not shown).

Our data also support the notion that a Slit-mediated Robo signal transduction mechanism is involved in proliferation since we observed very similar phenotypes in both Slit and Robo mutants. Given that the absence of Slit or Robo leads to increased proliferation, we were interested to know whether the converse was true, i.e., does the addition of Slit lead to a reduction in proliferation? To test this, we added Slit to GE dissociated cultures prepared from GAD67-GFP mice (in which all interneurons are GFP positive) and stained for the proliferation marker PH3. Since no functional differences are known to exist between the different Slit proteins, we decided to use a commercially available source of recombinant mouse Slit3 (mSlit3) in these experiments. We used a concentration of mSlit3 similar to that applied in experiments that demonstrated an effect of this molecule on the migration of cerebellar granule cells (Guan et al., 2007). In the absence of mSlit3, we observed that 27.97±1.98% of interneurons were PH3 positive, while in the presence of mSlit3 this value was significantly reduced to 7.36±0.67% ($p \leq 0.0001$) (Figs. 4J–L). These results suggest that mSlit3 is a potent inhibitor of cell proliferation in the GE. Similar results were obtained with human Slit1 and Slit2 (data not shown). As well as having an effect on interneuron proliferation, we also found that the presence of mSlit3 results in a significant decrease in neurite length, in agreement with a previous study that examined the effects of Slit1 on neuronal process branching and elongation (Sang et al., 2002).

The effect of Slit-Robo on cortical interneuron morphology

As well as investigating the role of Slit-Robo in cortical interneuron migration, we were also interested in evaluating

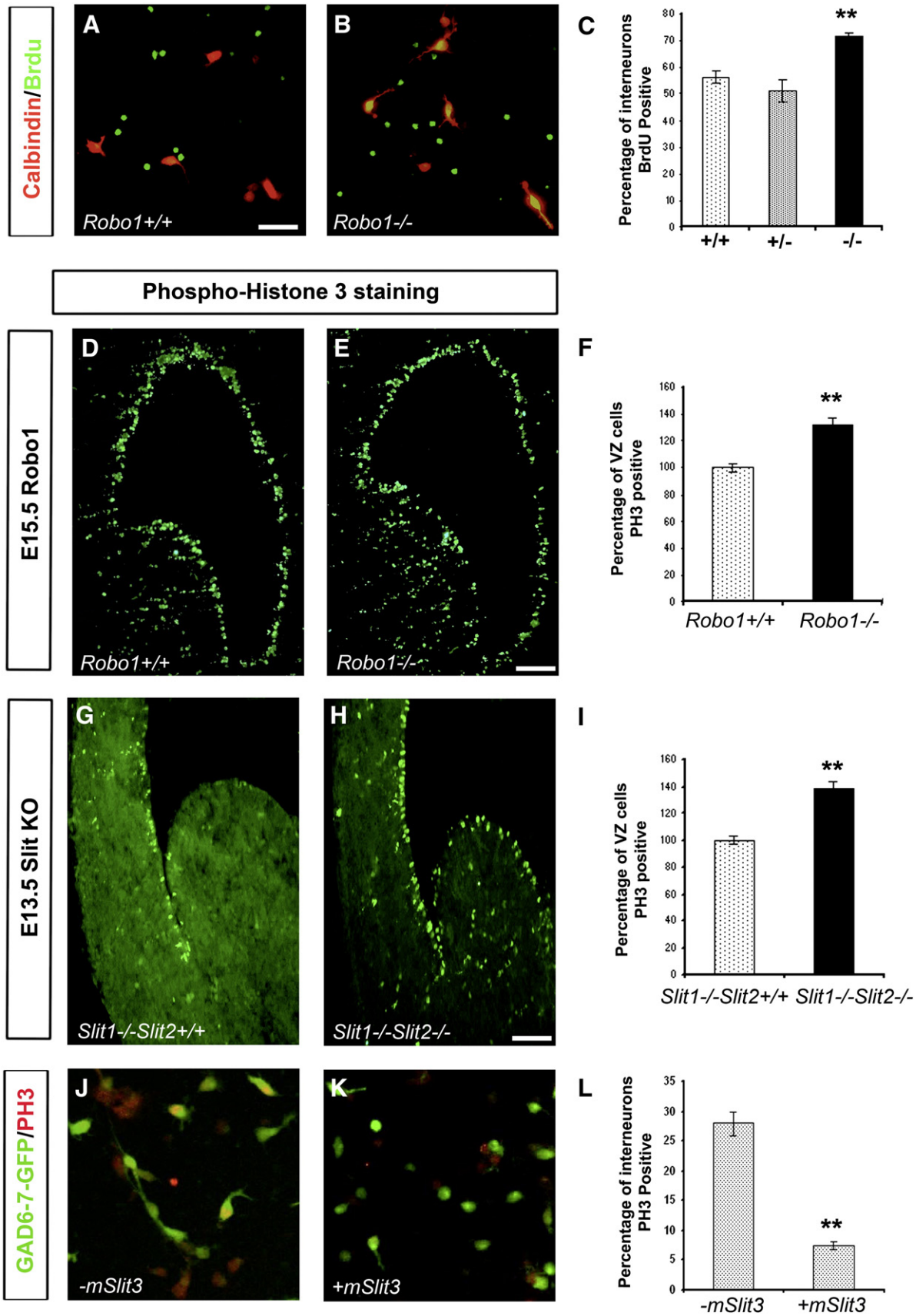
Calbindin/Brdu
A
Robo1+/+
B
Robo1-/-
C
Percentage of interneurons BrdU Positive
**
+/+
+/-
-/-
Phospho-Histone 3 staining
E15.5 Robo1
D
Robo1+/+
E
Robo1-/-
F
Percentage of VZ cells PH3 positive
**
Robo1+/+
Robo1-/-
E13.5 Slit KO
G
Slit1-/-Slit2+/+
H
Slit1-/-Slit2-/-
I
Percentage of VZ cells PH3 positive
**
Slit1-/-Slit2+/+
Slit1-/-Slit2-/-
GAD6-7-GFP/PH3
J
-mSlit3
K
+mSlit3
L
Percentage of interneurons PH3 Positive
**
-mSlit3
+mSlit3

their effects on the morphology of these cells. Previous reports have documented the effect of Slit and Robo on neuronal process length and branching in the CNS (Murray and Whitington, 1999; Wang et al., 1999; Ozdinler and Erzurumlu, 2002; Ma and Tessier-Lavigne, 2007) and in particular in GE explants and dissociated GABAergic cell cultures (Zhu et al., 1999; Sang et al., 2002). Here we wanted to study the effect of loss of Slit-Robo function on interneuron morphology *in vivo* using Robo and Slit mutant mice. Coronal sections taken through the middle (along the rostro-caudal axis) regions of the cortex of E15.5 mice were immunostained for calbindin, which labels neuronal cell bodies and processes. The total neurite length, number of neurite processes and number of branch points were quantified in Robo1$^{-/-}$ (n=6 Robo1$^{+/-}$, n=7 Robo1$^{-/-}$), Robo2$^{-/-}$ (n=4 Robo2$^{+/+}$, n=5 Robo2$^{-/-}$) and Slit (n=3 Slit1$^{-/-}$Slit2$^{+/+}$; n=3 Slit1$^{-/-}$Slit2$^{-/-}$) mutant mice (Fig. 5). Our analysis focused on the SP and SVZ/IZ steams of migrating interneurons, which contain the greatest number of readily quantifiable calbindin-positive cells at this age (30–50 neurons were measured per stream per animal). Our results showed that mean total process length was significantly longer in the SVZ/IZ of Robo1$^{-/-}$ mutants (Robo1$^{+/-}$, 46.6±1.8 μm; Robo1$^{-/-}$ 54.5±1.6 μm, $p \leq 0.0015$), but even more so in the SP compared to heterozygote littermates (Robo1$^{+/-}$ 43.4±1.8 μm; Robo1$^{-/-}$ 71.0±2.9 μm, $p \leq 8\times10^{-15}$) (Figs. 5A and J–K). Similarly, an increase in the number of neurites was seen in Robo1$^{-/-}$ mutant mice, both in the SVZ/IZ (Robo1$^{+/-}$ 1.51±0.04; Robo1$^{-/-}$ 1.86±0.04, $p \leq 2.1\times10^{-8}$) and SP (Robo1$^{+/-}$ 1.60±0.05, Robo1$^{-/-}$ 2.02±0.05, $p \leq 2.2\times10^{-8}$) compared to heterozygote littermates (Fig. 5B). Interestingly, an increase in the degree of branching was also observed in Robo1$^{-/-}$ animals in both SVZ/IZ (Robo1$^{+/-}$ 0.38±0.04; Robo1$^{-/-}$ 0.63±0.04, $p \leq 1.17\times10^{-5}$) and SP streams (Robo1$^{+/-}$ 0.51±0.05; Robo1$^{-/-}$ 0.86±0.05, $p \leq 2.3\times10^{-6}$) compared to heterozygote littermates (Fig. 5C). Identical patterns were seen in both Robo1 Exon 5 deleted and in the Robo1 Dulox transgenic lines, not only in terms of process length, but also in terms of number of neurites and branching (data not shown).

Similar morphological analysis performed in the cortices of Robo2$^{-/-}$ mice showed no major changes compared to wild-type littermates, except for an increase in process length in the SVZ/IZ (Figs. 5G–I). Thus, Robo1, but not Robo2, appears to have a significant effect on cortical interneurons, not only in terms of number but also on cellular morphology within the developing cortex.

Analysis of Slit1$^{-/-}$Slit2$^{+/+}$ animals revealed no significant alterations in interneuron morphology (neurite length and branching) as these parameters were identical to those obtained for Robo1 wild-type samples (Figs. 5A–C). However, analysis of Slit1$^{-/-}$Slit2$^{-/-}$ mice indicated a marked increase in process length, number of neurites and in branching, which is very similar to that obtained for Robo1$^{-/-}$ animals (Figs. 5D–F). Thus, absence of either Robo1 or both Slit1/2 molecules, but not Robo2, or Slit1, appears to have a pronounced effect on the morphology of migrating interneurons.

Discussion

Cortical GABAergic interneurons are generated in the ventral telencephalon and migrate tangentially to reach their final destinations in the neocortex and hippocampus (Métin et al., 2006). Because of their crucial role in cortical functions, as well as the impact that their abnormal development has on neurological conditions, the mechanisms underlying the migration of cortical interneurons are of considerable interest. Much has been learnt in recent years about the molecular cues that provide directionality to the migrating interneurons, and these include the actions of semaphorins and their receptors, neuregulins and the Slit-Robo proteins (Marín and Rubenstein, 2003; Métin et al., 2006; Andrews et al., 2007).

We have shown with immunohistochemistry that Robo1 and Robo2 are expressed throughout the cortical anlage and in the GE during the whole period of corticogenesis. The expression patterns of these receptors overlap to a large extent with one another and with the cortical interneuron marker calbindin, implying that these cells express Robo receptors. Our double labeling experiments have indeed, confirmed that the vast majority of cortical interneurons express Robo1 and Robo2. The expression patterns of Robo receptors are complementary to those of their ligands, the Slit molecules (Yuan et al., 1999; Bagri et al., 2002; Marillat et al., 2002; Whitford et al., 2002). Slit1 and Slit2 are expressed in the proliferative zones of the ventral telencephalon and in the septum during early and mid phases of corticogenesis and are thought to repel Robo expressing GABAergic interneurons to the cortex. *In vitro* explant assays have shown that the VZ of the LGE is repulsive to GABAergic neurons and that this repulsion is mediated by Slits (Zhu et al., 1999). Concomitant with their expression in the ventral telencephalon, Slit proteins show a well-defined pattern of expression in the developing cortex. Specifically, Slit1 is robustly expressed in the CP; Slit3 is restricted to the MZ, while Slit2 is weakly expressed in the VZ. The presence of a putative Slit gradient along the interneuron migratory routes suggests that Slit-Robo signaling may also play a role in the positioning

Fig. 4. The effects of Slit-Robo on cortical interneuron proliferation. Dissociated GE cultures prepared from E12.5 Robo1 wild-type (+/+), heterozygote (+/−) and homozygous mutant (−/−) mice were incubated with BrdU for 2 h and double-immunostained with anti-calbindin (red) and anti-BrdU antibodies (green) (A, B). The proportion of calbindin-positive cells that incorporated BrdU (appear yellow in panels A, B), graphically represented in panel C, is significantly increased in Robo1$^{-/-}$ mutant cultures compared to +/+ and +/− cultures. Immunohistological staining for phosphohistone 3 is shown in coronal sections taken through the brains of E15.5 Robo1$^{+/+}$ (D) and Robo1$^{-/-}$ (E), and E13.5 Slit1$^{-/-}$Slit2$^{+/+}$ (G) and Slit1$^{-/-}$Slit2$^{-/-}$ (H) animals. These are graphically represented in panels F and I, respectively, suggesting that there is increased staining in both Robo1 and Slit double mutants compared to control littermates. E12.5 wild-type (GAD67-GFP) dissociated GE cultures were incubated overnight in the absence (J) and presence (K) of 4 μg/ml mSlit3 and immunostained with anti-PH3 antibody (red). The proportion of green interneurons which are stained with PH3 (appear yellow in panels J, K) are graphically represented in panel L, which shows that mSlit3 has a dramatic effect on interneuron proliferation. Histograms show means and SEM. Students t-test **$p \leq 0.002$. Scale bars in panel A=80 μm in panels A, B, J and K. Scale bars in panels E and H=300 μm in panels D and G.

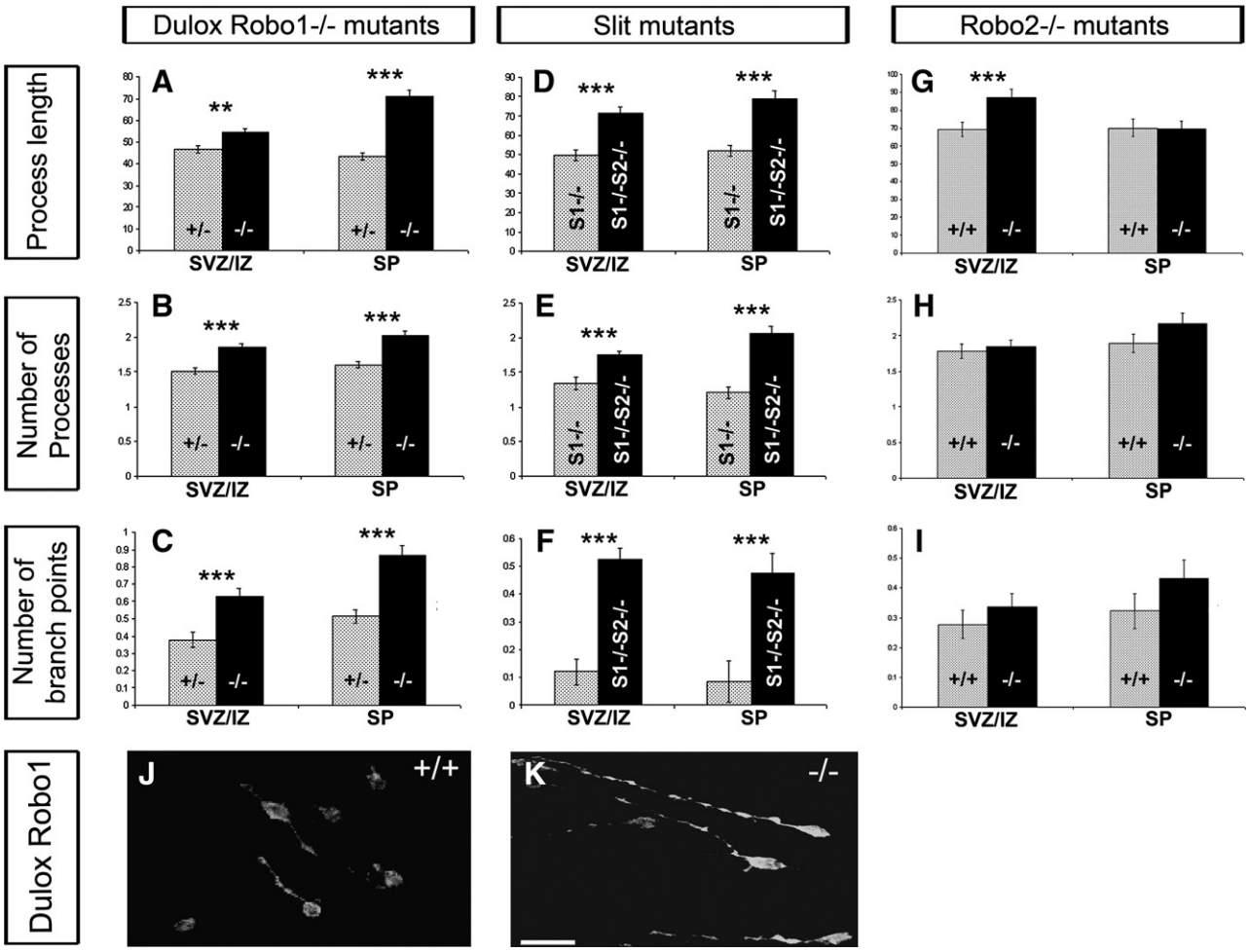

Fig. 5. Morphological differences in migrating interneurons in Robo and Slit mutants. Histograms representing morphological parameters of calbindin-positive cells in coronal sections taken through the cortices of Robo1$^{-/-}$ (A–C; Robo1$^{+/-}$white, Robo1$^{-/-}$ black), Slit (D–F; Slit1$^{-/-}$Slit2$^{+/+}$ white, Slit1$^{-/-}$Slit2$^{-/-}$ black) and Robo2$^{-/-}$ (G–I; Robo2$^{+/+}$ white, Robo2$^{-/-}$ black) mutant mice at E15.5. An increase in total neurite length (μm) was found in Robo1$^{-/-}$ (A), Robo2$^{-/-}$ (G) and Slit1$^{-/-}$Slit2$^{-/-}$ (D) animals compared to control littermates. This is also illustrated for Robo1 in panels J–K. We also noted an increase in the number of neurites (B, E) and the number of branch points (C, F) for both Robo1$^{-/-}$ and Slit1$^{-/-}$Slit2$^{-/-}$ animals compared to controls. Student's *t*-test $^{**}p<0.002$, $^{***}p<0.00001$. Scale bar in panel K = 20 μm for panels J and K.

of these tangential paths within the developing cortex. However, analysis of the migration and numbers of interneurons identified with a variety of markers at different embryonic stages showed no difference in the cortex between wild-type and Slit1$^{-/-}$Slit2$^{-/-}$ double- and Slit1$^{-/-}$Slit2$^{-/-}$netrin$^{-/-}$ triple mutants (Marín et al., 2003). These observations suggest that Slit1 and Slit2 are not necessary for the tangential migration of interneurons to the cortex. However, these proteins appear to regulate neuronal migration within the basal telencephalon (Marín et al., 2003).

Although Slit mutants do not show any difference in the number and distribution of cortical interneurons (shown here and Marín et al., 2003), we noted a marked increase in the number of such cells in all layers in Robo1$^{-/-}$ mutants throughout corticogenesis and in adulthood. The fact that such phenotype was not observed in the Slit1$^{-/-}$Slit2$^{-/-}$ animals suggests that this may be a Slit independent event, or that an unidentified member of the Slit family of molecules may be involved. We speculated that the cell increase could be due to a change in migration rate or a consequence of failure to respond to inhibitory cues, normally imposed by the presence of Slit in the cortex, or due to changes in proliferation/apoptosis. We have demonstrated here that the increased number of interneurons in the cortex of Robo1$^{-/-}$ animals is, at least in part, due to increased proliferation in the GE. Interestingly, we observed a similar increase in proliferation in Slit1$^{-/-}$Slit2$^{-/-}$ mutants, suggesting that Slit-Robo signalling mechanisms are involved in regulating cell division.

While Slit has been shown to play a role in asymmetrical cell division in *Drosophila* (Mehta and Bhat, 2001), this is the first report of Slit-Robo signaling having a direct effect on cell proliferation in a neuronal cell type in vertebrates. It is pertinent to note that abundant evidence points to an active role for Slit-Robo signaling in tumor development. Specifically, tumor suppressor gene activity has been proposed for Slit2 and Robo1 in lung and breast cancer (Sundaresan et al., 1998), and several studies have shown that both genes are frequently inactivated in lung adenocarcinomas and lymphomas by

methylation of the gene promoters (Dallol et al., 2002; Xian et al., 2004). Moreover, Xian and colleagues (2004) have demonstrated that Dutt1/Robo1 transgenic mice show a higher incidence of lymphomas and carcinomas than wild-type littermates, suggesting that *Dutt1/Robo1* acts as a tumor suppressor gene.

Although we observed an increase in proliferation in Slit1$^{-/-}$Slit2$^{-/-}$ mutant mice, we did not note a corresponding increase in the number of interneurons entering the cortex. One possible explanation may be that the continued presence of Slit3 in the cortices of Slit1$^{-/-}$Slit2$^{-/-}$ mutant mice prevents interneurons from migrating into the cortex prematurely. Secondly, we observed recently that interneurons migrate into the normally repulsive striatum in Robo1$^{-/-}$ mutants (Andrews et al., 2006). Thus, we speculated that some interneurons take a "short-cut" through this region, which could explain their increased number in the cortices of Robo1$^{-/-}$ mice, unlike the Slit1$^{-/-}$Slit2$^{-/-}$ animals where interneurons have not been shown to enter the striatal region (Marín et al., 2003). Thus, the different migratory paths taken by interneurons in Slit and Robo1 mutants could account for the differences seen in the number of cells entering the cortex. We are actively testing these hypotheses at present.

There are several lines of evidence to suggest that Slit-Robo proteins play a role in neuronal process elongation and branching in a number of developing systems (Ozdinler and Erzurumlu, 2002; Ma and Tessier-Lavigne, 2007). In more pertinent studies that utilized MGE explants and cortical cell cultures (Sang et al., 2002; Sang and Tan, 2003; Whitford et al., 2002), Slit was found to promote process elongation and branching on cortical interneurons. At first glance, these results seem to contradict our *in vivo* findings. However, not all interneuron cohorts respond to Slit in a similar fashion, as the work of Sang and colleagues (2002, 2003) has indicated that the response varies according to the age of the dissociated cells. Whereas interneuron cultures established from early stages (E13.5 and E15.5) showed suppressed neurite growth, in line with our observations in E15.5 Slit mutants, interneurons cultured from E17.5 brains responded to Slit by increasing neurite branching.

In summary, we found that the majority of cortical interneurons express both Robo1 and Robo2 and that absence of Robo1, but not Robo2 or Slit proteins, leads to an increase in the number of interneurons migrating to the cortex from the ventral telencephalon. This increase may be attributed, at least in part, to increased cell proliferation. Analysis of the morphology of cortical interneurons in the same mutants revealed that lack of Robo1 or Slit1/Slit2, but not Robo2 or Slit1, has a pronounced effect on process elongation and branching. These observations suggest that the same Robo1–Slit1/Slit2 signal transduction mechanism is utilized within the cortex to regulate interneuron morphology.

Acknowledgments

We are grateful to Drs. Clare Faux and Gaelle Friocourt for helpful comments in the preparation of the manuscript. We are also grateful to Dr. M. Tessier-Lavigne for supplying Slit mutants and to Drs. Y. Yanagawa and K. Obata for giving us the *GAD67-GFP* mice used in this study. The work was supported by a Wellcome Trust Grant Programme Grant (074549).

Appendix A. Supplementary data

Supplementary data associated with this article can be found, in the online version, at doi:10.1016/j.ydbio.2007.10.052.

References

Andrews, W., Liapi, A., Plachez, C., Camurri, L., Zhang, J., Mori, S., Murakami, F., Parnavelas, J.G., Sundaresan, V., Richards, L.J., 2006. Robo1 regulates the development of major axon tracts and interneuron migration in the forebrain. Development 133, 2243–2252.

Andrews, W.D., Barber, M., Parnavelas, J.P., 2007. Slit-Robo interactions during cortical development. J. Anat. 221, 188–189.

Bagri, A., Marín, O., Plump, A.S., Mak, J., Pleasure, S.J., Rubenstein, J.L., Tessier-Lavigne, M., 2002. Slit proteins prevent midline crossing and determine the dorsoventral position of major axonal pathways in the mammalian forebrain. Neuron 33, 233–248.

Cavanagh, J.F., Mione, M.C., Pappas, I.S., Parnavelas, J.G., 1997. Basic fibroblast growth factors prolongs the proliferation of rat cortical progenitor cells in vitro without altering their cell cycle parameters. Cereb. Cortex 4, 293–302.

Cobos, I., Calcagnotto, M.E., Vilaythong, A.J., Thwin, M.T., Noebels, J.L., Baraban, S.C., Rubenstein, J.L., 2005. Mice lacking *Dlx1* show subtype-specific loss of interneurons, reduced inhibition and epilepsy. Nat. Neurosci. 8, 1059–1068.

Corbin, J.G., Nery, S., Fishell, G., 2001. Telencephalic cells take a tangent: non-radial migration in the mammalian forebrain. Nat. Neurosci. 1177–1182 (Suppl.).

Dallol, A., Fernandes Da Silva, N., Viacava, P., Minna, J.D., Bieche, I., Maher, E.R., Latif, F., 2002. Slit2, a human homologue of the *Drosophila Slit2* gene, has tumour suppressor activity and is frequently inactivated in lung and breast cancers. Cancer Res. 62, 5874–5880.

Friocourt, G., Liu, J.S., Antypa, M., Rakic, S., Walsh, C.A., Parnavelas, J.G., 2007. Both doublecortin and doublecortin-like kinase play a role in cortical interneuron migration. J. Neurosci. 27, 3875–3883.

Guan, C.B., Xu, H.T., Jin, M., Yuan, X.B., Poo, M.M., 2007. Long-range Ca^{2+} signaling from growth cone to soma mediates reversal of neuronal migration induced by slit-2. Cell 129, 385–395.

Hu, H., 1999. Chemorepulsion of neuronal migration by Slit2 in the developing mammalian forebrain. Neuron 23, 703–711.

Kumar, S.S., Buckmaster, P.S., 2006. Hyperexcitability, interneurons, and loss of GABAergic synapses in entorhinal cortex in a model of temporal lobe epilepsy. J. Neurosci. 26, 4613–4623.

López-Bendito, G., Flames, N., Ma, L., Fouquet, C., Di Meglio, T., Chedotal, A., Tessier-Lavigne, M., Marín, O., 2007. Robo1 and Robo2 cooperate to control the guidance of major axonal tracts in the mammalian forebrain. J. Neurosci. 27, 3395–3407.

Lu, W., van Eerde, A.M., Fan, X., Quintero-Rivera, F., Kulkarni, S., Ferguson, H., Kim, H.G., Fan, Y., Xi, Q., Li, Q.G., Sanlaville, D., Andrews, W., Sundaresan, V., Bi, W., Yan, J., Giltay, J.C., Wijmenga, C., de Jong, T.P., Feather, S.A., Woolf, A.S., Rao, Y., Lupski, J.R., Eccles, M.R., Quade, B.J., Gusella, J.F., Morton, C.C., Maas. R, L., 2007. Disruption of ROBO2 is associated with urinary tract anomalies and confers risk of vesicoureteral reflux. Am. J. Hum. Genet. 80, 616–632.

Ma, L., Tessier-Lavigne, M., 2007. Dual branch-promoting and branch-repelling actions of Slit/Robo signaling on peripheral and central branches of developing sensory axons. J. Neurosci. 27, 6843–6851.

Mallet, N., Ballion, B., Le Moine, C., Gonon, F., 2006. Cortical inputs and GABA interneurons imbalance projection neurons in the striatum of Parkinsonian rats. J. Neurosci. 26, 3875–3884.

Marillat, V., Cases, O., Nguyen-Ba-Charvet, K.T., Tessier-Lavigne, M., Sotelo, C., Chedotal, A., 2002. Spatiotemporal expression patterns of slit and robo genes in the rat brain. J. Comp. Neurol. 442, 130–155.

Marín, O., Rubenstein, J.L., 2003. Cell migration in the forebrain. Annu. Rev. Neurosci. 26, 441–483.

Marín, O., Plump, A.S., Flames, N., Sanchez-Camacho, C., Tessier-Lavigne, M., Rubenstein, J.L., 2003. Directional guidance of interneuron migration to the cerebral cortex relies on subcortical Slit1/2-independent repulsion and cortical attraction. Development 130, 1889–1901.

Mehta, B., Bhat, K.M., 2001. Slit signaling promotes the terminal asymmetric division of neural precursor cells in *Drosophila* CNS. Development 128, 3161–3168.

Métin, C., Baudoin, J.P., Rakic, S., Parnavelas, J.G., 2006. Cell and molecular mechanisms involved in the migration of cortical interneurons. Eur. J. Neurosci. 23, 894–900.

Murray, M.J., Whitington, P.M., 1999. Effects of roundabout on growth cone dynamics, filopodial length, and growth cone morphology at the midline and throughout the neuropile. J. Neurosci. 19, 7901–7912.

Nadarajah, B., Parnavelas, J.G., 2002. Modes of neuronal migration in the developing cerebral cortex. Nat. Rev., Neurosci. 3, 423–432.

Ozdinler, P.H., Erzurumlu, R.S., 2002. Slit2, a branching-arborization factor for sensory axons in the mammalian CNS. J. Neurosci. 22, 4540–4549.

Plump, A.S., Erskine, L., Sabatier, C., Brose, K., Epstein, C.J., Goodman, C.S., Mason, C.A., Tessier-Lavigne, M., 2002. Slit1 and Slit2 cooperate to prevent premature midline crossing of retinal axons in the mouse visual system. Neuron 33, 219–232.

Poirier, K., Van Esch, H., Friocourt, G., Saillour, Y., Bahi, N., Backer, S., Souil, E., Castelnau-Ptakhine, I., Beldjord, C., Francis, F., Bienvenu, T., 2004. Neuroanatomical distribution of ARX in brain and its localisation in GABAergic neurons. Mol. Brain Res. 122, 35–46.

Sang, Q., Tan, S.S., 2003. Contact-associated neurite outgrowth and branching of immature cortical interneurons. Cereb. Cortex 13, 677–683.

Sang, Q., Wu, J., Rao, Y., Hsueh, Y.P., Tan, S.S., 2002. Slit promotes branching and elongation of neurites of interneurons but not projection neurons from the developing telencephalon. Mol. Cell. Neurosci. 21, 250–265.

Sloviter, R.S., 1987. Decreased hippocampal inhibition and a selective loss of interneurons in experimental epilepsy. Science 235, 73–76.

Sundaresan, V., Chung, G., Heppel-Parton, A., Xiong, J., Grundy, C., Roberts, I., James, L., Cahn, A., Bench, A., Douglas, J., Minna, J., Sekido, Y., Lerman, M., Latif, F., Bergh, J., Li, H., Lowe, N., Ogilvie, D., Rabbitts, P., 1998. Homozygous deletions at 3p12 in breast and lung cancer. Oncogene 17, 1723–1729.

Tamamaki, N., Yanagawa, Y., Tomioka, R., Miyazaki, J., Obata, K., Kaneko, T., 2003. Green fluorescent protein expression and colocalization with calretinin, parvalbumin, and somatostatin in the GAD67-GFP knock-in mouse. J. Comp. Neurol. 467, 60–79.

Thomaidou, D., Mione, M.C., Cavanagh, J.F., Parnavelas, J.G., 1997. Apoptosis and its relation to the cell cycle in the developing cerebral cortex. J. Neurosci. 17, 1075–1085.

Wang, K.H., Brose, K., Arnott, D., Kidd, T., Goodman, C.S., Henzel, W., Tessier-Lavigne, M., 1999. Biochemical purification of a mammalian slit protein as a positive regulator of sensory axon elongation and branching. Cell 96, 771–784.

Whitford, K.L., Marillat, V., Stein, E., Goodman, C.S., Tessier-Lavigne, M., Chedotal, A., Ghosh, A., 2002. Regulation of cortical dendrite development by Slit-Robo interactions. Neuron 33, 47–61.

Wu, W., Wong, K., Chen, J., Jiang, Z., Dupuis, S., Wu, J.Y., Rao, Y., 1999. Directional guidance of neuronal migration in the olfactory system by the protein Slit. Nature 400, 331–336.

Xian, J., Clark, K.J., Fordham, R., Pannell, R., Rabbitts, T.H., Rabbitts, P.H., 2001. Inadequate lung development and bronchial hyperplasia in mice with a targeted deletion in the Dutt1/Robo1 gene. Proc. Natl. Acad. Sci. U. S. A. 98, 15062–15066.

Xian, J., Aitchison, A., Bobrow, L., Corbett, G., Pannell, R., Rabbitts, T.H., Rabbitts, P.H., 2004. Targeted disruption of the 3p12 gene, *Dutt1/Robo1*, predisposes mice to lung adenocarcinomas and lymphomas with methylation of the gene promoter. Cancer Res. 64, 6432–6437.

Yuan, W., Zhou, L., Chen, J.H., Wu, J.Y., Rao, Y., Ornitz, D.M., 1999. The mouse SLIT family: secreted ligands for ROBO expressed in patterns that suggest a role in morphogenesis and axon guidance. Dev. Biol. 212, 290–306.

Zhu, Y., Li, H., Zhou, L., Wu, J.Y., Rao, Y., 1999. Cellular and molecular guidance of GABAergic neuronal migration from an extracortical origin to the neocortex. Neuron 23, 473–485.